Title	Image-Based Machine Learning of In Situ Captured Images of Die-Workpiece Interface in Forging
Author(s)	Matsumoto, Ryo; Kunisawa, Shusuke; Nakamura, Yusaku et al.
Citation	Defect and Diffusion Forum. 2025, 441(9), p. 39-43
Version Type	AO
URL	https://hdl.handle.net/11094/100688
rights	
Note	

Image-Based Machine Learning of *In Situ* Captured Images of Die–Workpiece Interface in Forging

Ryo Matsumoto[1,a*], Shusuke Kunisawa[1], Yusaku Nakamura[1] and Hiroshi Utsunomiya[1,b]

[1]Division of Materials and Manufacturing Science, Osaka University, 2-1 Yamadaoka, Suita, Osaka 565-0871, Japan

[a]ryo@mat.eng.osaka-u.ac.jp, [b]uts@mat.eng.osaka-u.ac.jp

Keywords: Forging, Extrusion, Lubrication, Image analysis, Machine learning

Abstract. The lubricant thickness in cold forging was estimated by machine learning of the *in situ* captured images of the die–workpiece contact interface. The images were *in situ* captured by a high-speed camera from the backside of the transparent glass die during forging of commercially pure aluminum workpiece. On the other hand, the images of the lubricated workpiece were individually captured as training images for random forest with classification. The classification accuracy of the lubricant thickness was confirmed to be approximately 75% (classification ability: 5–10 μm in lubricant thickness) in the training images with 22,500 px (50 px/mm). The *in situ* captured images of the die–workpiece contact interface during forging were classified by random forest using the training images. The estimated lubricant thickness of the *in situ* captured image almost agreed with the lubricant thickness estimated from the mean brightness value of the *in situ* captured image.

Introduction

Partial use of transparent glass in die is a well-known technique for *in situ* (direct) observation of die–workpiece contact interface during forming [1]. The die–workpiece contact interface was observed from the backside of the glass by a camera. In recent research works, lubricant flow during micro bending and ironing using glass die with micro dimples [2], the behavior of lubricant with fine-ceramic particles during cold ironing [3], and the lubricating behavior during cold drawing using the fluorescence method [4] were *in situ* observed. We also reported the *in situ* observation of roll–strip contact interface during cold rolling with Ptolemaic rolling apparatus [5] and the *in situ* observation of re-lubricating behavior during oscillation forging [6]. In many cases of the research works concerning the *in situ* observation, the captured images are not quantitatively analyzed by image processing but qualitatively analyzed by visual inspection.

On the other hand, machine learning techniques are applied in the field of metal forming. Concerning image-based machine learning, surface defects such as crack and hole were detected in rolled strip by the captured images of rolled strip [7]. The image-based machine learning may be an effective tool for analyzing quantitatively and objectively the features in the captured images.

For analyzing lubricating behavior during cold forging, machine learning is performed on the captured images of the lubricated workpiece in this study. The influence of the machine learning conditions on the classification accuracy of the lubricant thickness is investigated by using the training data of the captured images of the workpiece. Then the lubricant thickness is estimated from the *in situ* captured images of the die–workpiece contact interface.

In Situ Observation Conditions of Die–Workpiece Contact Interface during Forging

Die Layout and *In Situ* Observation Conditions. Fig. 1 shows the appearance of the apparatus and the die layout for *in situ* observation of the glass die–workpiece contact interface in forging. The apparatus was used in our previous research work for the *in situ* observation of the contact interface, and the dimensions of the dies and the workpiece were described in our previous report [6]. The transparent glass for the observation window was made of ceramic glass (Ohara Inc.: NANOCERAM). The disk-shaped glass with 12.0 mm in diameter and 5.0 mm in thickness was inserted into the tapered section of the lower die.

The contact interface was observed through a straight hole (minimum diameter: 4.0 mm) in the lower die and case from the backside of the transparent glass. The glass die–workpiece contact interface was captured by a high-speed camera with a white LED light source. The captured area and resolution were 3.0 mm × 4.0 mm and 600 pixels × 800 pixels (200 px/mm) in the parallel x horizontal directions with the tapered surface in the lower die, respectively.

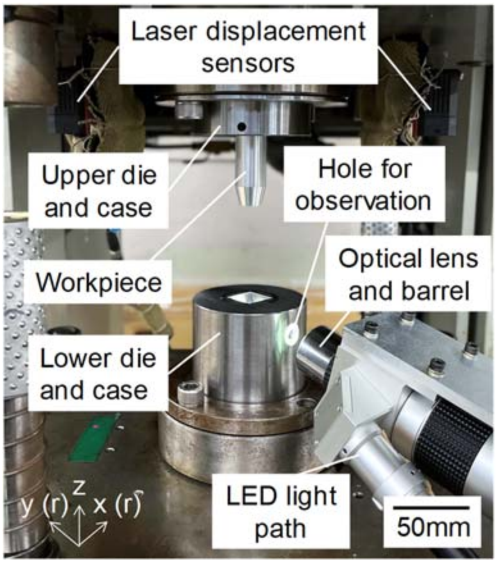

(a) Appearance.

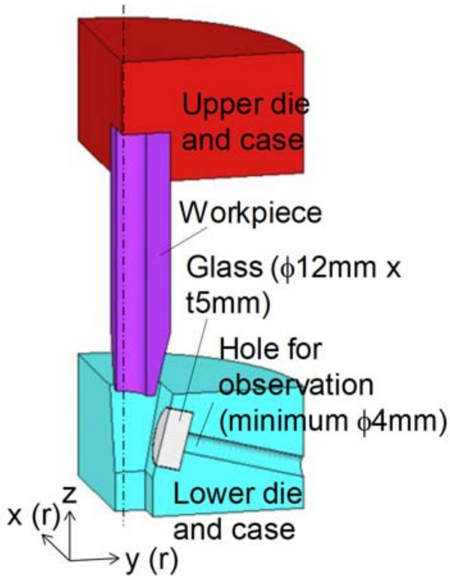

(b) Die and workpiece layout.

Fig. 1 Appearance of apparatus and die layout for *in situ* observation of glass die–workpiece contact interface in forging.

Forging Conditions. JIS A1070 aluminum hollow cylindrical workpiece (Al ≥ 99.7 mass%, Vickers hardness: 36.8 HV0.2) was forged in two stages at room temperature on a link-type servo press. The first stage of forging was for preform of the workpiece with a forging stroke of s_1 = 12 mm, while the second stage of forging was for the *in situ* observation of the die–workpiece contact interface with a forging stroke of s_2 = 13 mm (total forging stroke: s_1+s_2 = 25 mm).

Before the second stage of forging, polybutene (280 mm^2/s at 313 K) with 5 vol% oil-soluble black colorant was applied to the tapered section of the workpiece with approximately 80 μm in mean thickness using a syringe. Hereafter, polybutene with colorant was simply described as lubricant.

Image Analysis Procedures by Machine Learning

Photographic Conditions of Training Images. The training images of the lubricated workpiece for machine learning were prepared as follows. (1) The lubricant was applied to the tapered section of the workpiece forged with s_1+s_2 = 25 mm. (2) The workpiece was inserted into the lower die. (3) The surface of the workpiece was captured through the observation hole in the lower die under the same photographic conditions with the *in situ* observation. Here, the lubricant film with thickness of 0–80 μm was formed at a maximum of 11 classes with classification intervals of 5 μm or 10 μm. Maximum 100 training images were prepared for each lubricant thickness. The lubricant thickness was controlled by the application volume of the lubricant and the application area of the workpiece.

Fig. 2 shows the examples of the training images of the lubricated workpiece for machine learning. The training image of thin lubricant thickness was bright (brightness value: high), while that of thick lubricant thickness was dark (brightness value: low). The lubricant thickness was not uniform in the analysis area, and the mean coefficient of variation of the brightness value was 0.33 in all captured images with lubricant thickness of 0–80 μm. The mean lubricant thickness was labeled as the lubricant thickness in the analysis.

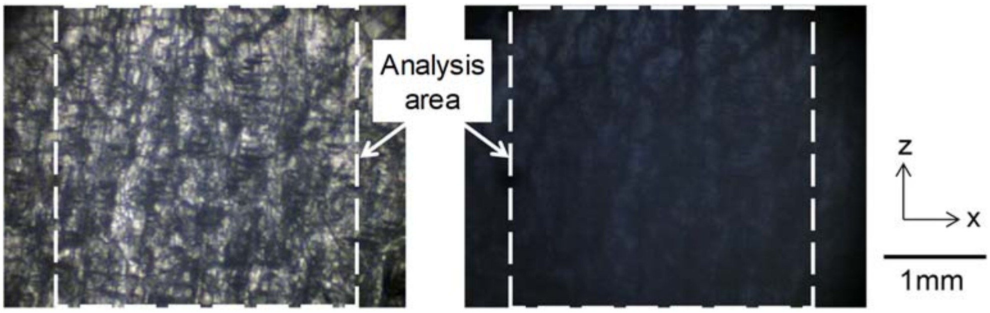

(a) Mean lubricant thickness: 10 μm (mean bv: 101, cov of bv: 0.36).

(b) Mean lubricant thickness: 80 μm (mean bv: 41, cov of bv: 0.19).

Fig. 2 Examples of training image of workpiece (bv: brightness value, cov: coefficient of variation).

Image Analysis Conditions. The RGB value of each pixel coordinate in the color captured image was converted to the brightness values between 0 (black) and 255 (white). The brightness value was set as explanatory variable. The *in situ* captured images of the die–workpiece contact interface with lubricant during forging were classified by random forest using the training images. The importance of each explanatory variable for classification of the lubricant thickness was also calculated. In the random forest, 70% of the training images were set as the training data, while 30% of the training images were set as the validation data. The images were classified by the cross-validation in 1,000 decision trees with less than 10 layers.

The analysis area of the captured image was set to 3.0 mm in z direction and 3.0 mm in x direction, excluding both ends in the x direction (see Fig. 2). The basic resolution of the training images and the *in situ* captured images was degraded with 150 pixels × 150 pixels (50 px/mm). The basic conditions of the training images were 11 classes with classification intervals of 5 μm or 10 μm and 50 images for each film thickness in the maximum film thickness with 80 μm.

Classification Accuracy in Machine Learning of Training Images

Fig. 3 shows the relationship between the classification accuracy of the lubricant thickness and the number of images for each lubricant thickness in the training images. Here, the classification accuracy is the probability that the validation images are correctly classified into the class of the lubricant thickness. The classification accuracy increased with the number of images for each lubricant thickness, and the classification accuracy was approximately 75% for 50 images and 100 images for each lubricant thickness. In order to increase the classification accuracy to over 90%, several hundred or more images for each lubricant thickness, or images with clear characteristics for each lubricant thickness, is expected to be required.

The relationship between the classification accuracy of the lubricant thickness and the number of classes of the lubricant thickness in the training images is shown in Fig. 4. Here, the images with lubricant thicknesses of 0 μm and 80 μm were absolutely included at each classification analysis. The classes were selected at equal class intervals of the lubricant thickness according to the number of classes. The classification accuracy decreased as the number of classes increased, however the classification accuracy was kept to be approximately 75% in over five classes (class intervals: thinner than 20 μm in lubricant thickness). Considering the mean brightness value was changed by 5–10 with a change of 5 μm in lubricant thickness under the photographic conditions, the difference of 5–10 in brightness value is suggested to be classified with approximately 75% accuracy under 11 classes with classification intervals of 5 μm.

From the above results, it is concluded that the classification accuracy is approximately 75% with 5–10 μm of classification ability in lubricant thickness for the captured images with 50 px/mm under the photographic conditions.

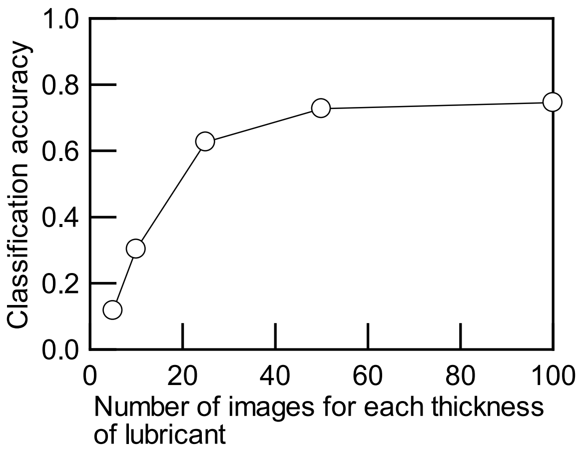

Fig. 3 Relationship between classification accuracy of lubricant thickness and number of images for each lubricant thickness in training images.

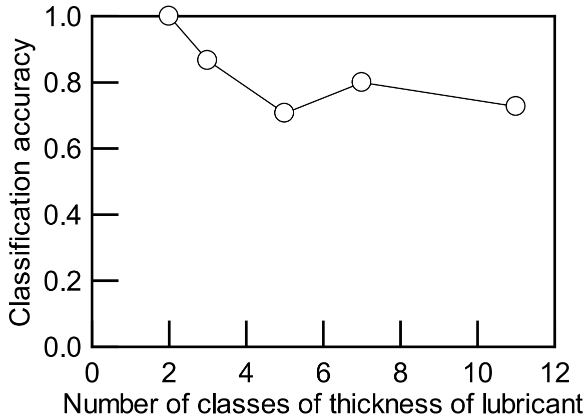

Fig. 4 Relationship between classification accuracy of lubricant thickness and number of classes of lubricant thickness in training images.

Estimation of Lubricant Thickness by Machine Learning of *In Situ* Captured Images of Die–Workpiece Contact Interface during Forging

Fig. 5 shows the predicted results of the lubricant thickness in the *in situ* captured images of die–workpiece contact interface during forging. Here, the classification interval of the lubricant thickness was 5 μm in lubricant thickness of 10–40 μm in the prediction by machine learning. For comparison, the lubricant thickness predicted from the mean brightness value of the *in situ* captured image was also plotted on the basis of the mean brightness value–lubricant thickness relationship in the training images [6]. The relationship was approximated by the Beer–Lambert law [8] in the training images. Generally good agreement of the predicted lubricant thickness between the machine leaning and the Beer–Lambert approximation was obtained. No specific pixel point (location) for the brightness value was found in the importance of brightness value for classification of the lubricant thickness. Therefore, the classification of the lubricant thickness was not strongly affected by the brightness value at a specific pixel point, so that it is concluded that the lubricant thickness predicted by the machine learning almost agrees with the lubricant thickness based on the mean brightness value.

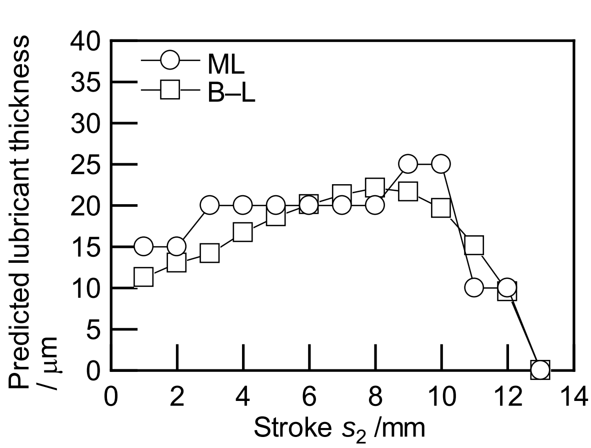

Fig. 5 Predicted results of lubricant thickness in *in situ* captured images of die–workpiece contact interface during forging (ML: prediction by machine learning, B–L: prediction by mean brightness value–lubricant thickness relationship).

The lubricating behavior during forging was suggested from the predicted lubricant thickness as follows. Due to the contact of the lubricated workpiece with the lower die at the start of forging (s_2 = 0 mm), much of the lubricant was squeezed out to the outside of the *in situ* observed area. As the contacting pressure between the lower die and the workpiece increased at s_2 = 0–10 mm, the contact surface of the workpiece was slightly concaved by trapping the lubricant at the center of the lower die–workpiece contact area, which was the *in situ* observed area. As the results, the lubricant thickness increased at s_2 = 0–10 mm. On the other hand, the lubricant was stretched by extruding the workpiece toward the forward at s_2 = 10–13 mm, resulting in the lubricant thickness thinning.

Conclusions

In this study, machine learning of the captured images of the lubricated workpiece was performed for estimation of the lubricant thickness. Following conclusions were obtained.

1) The classification accuracy of the lubricant thickness was confirmed to be approximately 75% (classification ability: 5–10 μm in thickness) in the training images with 22,500 px (50 px/mm).
2) The *in situ* captured images of the die–workpiece contact interface with lubricant during forging were classified by using the training images. The estimated lubricant thickness almost agreed with the lubricant thickness estimated from the mean brightness value of the *in situ* captured image.

Acknowledgements

This work was financially supported in part by the Amada Foundation (AF-2022006-B2) and the Mould Technology Promotion Foundation.

References

[1] A. Azushima, Direct observation of contact behavior to interpret the pressure dependence of the coefficient of friction in sheet metal forming, CIRP Ann. Manuf. Technol., 44-1 (1995) 209–212.

[2] T. Shimizu, H. Kobayashi, J. Vorholt, M. Yang, Lubrication analysis of micro-dimple textured die surface by direct observation of contact interface in sheet metal forming, Metals, 9-9 (2019) 917.

[3] Y. Abe, K. Ichimura, K. Mori, In-situ observation of behavior of containing ceramic particles in lubricant in ironing using glass die, Proc. 71st Jpn. Jt. Conf. Technol. Plast., (2020), 201–212.

[4] K. Hirade, T. Morishima, A. Yanagida, Direct measurement of lubricant film thickness during flat drawing process by fluorescence method, Proc. 74th Jpn. Jt. Conf. Technol. Plast., (2023), 59–60.

[5] H. Utsunomiya, Y. Terada, K. Ono, R. Matsumoto, *In situ* observation of the interface between a roll and a sheet in flat rolling process, CIRP Ann. Manuf. Technol., 71-1 (2022) 245–248.

[6] R. Matsumoto, Y. Nakamura, H. Utsunomiya, *In situ* observation of re-lubrication of die–workpiece interface during forging with ram pulsation, J. Manuf. Process., 101 (2023) 675–686.

[7] Z. Hao, Z. Li, F. Ren, S. Lv, H. Ni, Strip steel surface defects classification based on generative adversarial network and attention mechanism, Metals, 12-2 (2022) 311.

[8] J.W. Verhoeven, Glossary of terms used in photochemistry (IUPAC Recommendations 1996), Pure and Applied Chemistry, 68-12 (1996) 2230.